

This article is copyrighted as indicated in the article. Reuse of AIP content is subject to the terms at: <http://scitation.aip.org/termsconditions>. Downloaded to IP: 128.138.41.170 On: Tue, 14 Jul 2015 12:54:25

Proposal for III-V ordered alloys with infrared band gaps

Su-Huai Wei and Alex Zunger

Solar Energy Research Institute, Golden, Colorado 80401

(Received 21 February 1991; accepted for publication 5 April 1991)

It is shown theoretically that the recently observed spontaneous ordering of III-V alloys that yields alternate monolayer (111) superlattices provides the opportunity for achieving infrared band gaps in systems such as $(InAs)_1(InSb)_1$ and $(GaSb)_1(InSb)_1$. A substantial reduction in the *direct* band gap is predicted to result from the L -point folding that repel the Γ band-edge states.

Substantial effort has recently been focused on developing semiconductor materials for infrared (IR) devices in the model system $In_xGa_{1-x}As$ where the x dependence of intersubband absorption in tunnelling III-V superlattices,² four general physical principles have been previously utilized to directly shift band gaps into the IR spectral

of the constituents (AC) is lower in energy than the VBM of the other (BC); in this type of band lineup, the superlattice gap is determined by the difference in the valence-band edge of the constituents. This approach has been proposed by Arch *et al.*⁸ for AC = InAs and BC = GaSb. Like in (iii) above, here, too, relatively thick layer would be required to counteract

(i) *Bulk alloying.* In this simple approach one uses the fact that alloy band gaps vary smoothly and continuously with composition (often with a parabolic deviation from linearity), and seeks a combination of mutually soluble semiconductors (e.g., $In_xGa_{1-x}As$) and large gap BC (e.g., CdTe) semiconductors that produces a $(SG)_{1-x}(LG)_x$ alloy with a desired IR gap.

II' band arrangement, thick layers deteriorate severely the intensity of optical absorption due to increased separation between electrons and holes. To reduce the layer thickness needed, the principle of "strain-induced band-gap reduc-

(ii) *Superlattice quantum confinement without strain.* The basic idea here is to take a semiconductor with a very

Mailhiot⁹ for AC = InAs and BC = $Ga_{1-x}In_xSb$. This system was grown successfully by Chow *et al.*¹⁰ where far-infrared photoluminescence was observed.

We discuss here a different principle of achieving infrared band gaps with III-V materials, namely, "ordering

larger gap (LG). For small layer thicknesses (p,q), quant-

ization effects (SGSI) oriented superlattices considered

thus increasing the superlattice gap above that of pure SG

point) folds into the Brillouin zone center. This leads to a

gap and small lattice constant (SGSL) and layer it coherently with a material having a larger gap and larger lattice constant (LGLL), forming a strained-layer (SGSL)_p/ (LGLL) superlattice. Coherence of SGSI with LGLL

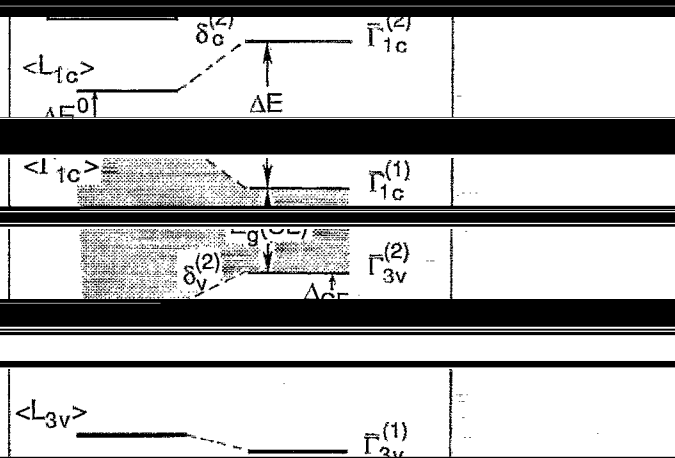


FIG. 1. Schematic plot of energy level shift at $\bar{\Gamma}$ of a typical III-V alloy

herently the misfit strain limits the maximum thickness that can be used.

(iv) *Superlattice-induced band inversion.* The basic

TABLE I. Calculated energy differences (eV) between the coupling states $\langle L_{1c} \rangle$ and $\langle \Gamma_{1c} \rangle$ before (ΔE^0) and after (ΔE) the perturbation potential is turned on. Values in parenthesis are for unrelaxed structures.

	GaAs/InAs	GaAs/InSb	GaAs/GaSb	InAs/InSb
$\Delta E^0 = \langle L_{1c} \rangle - \langle \Gamma_{1c} \rangle$	0.99	0.68	0.47	1.0
$\Delta E = \bar{\Gamma}_{1c}^{(2)} - \bar{\Gamma}_{1c}^{(1)}$	1.43 (1.22)	1.22 (1.02)	1.77 (1.28)	1.84 (1.39)
$R = \Delta E - \Delta E^0$	0.44 (0.23)	0.54 (0.34)	1.30 (0.81)	0.84 (0.39)

reduces the direct band gap, thus overwhelming the opposite effect of δV on the superlattice states. The δE^0 values in Table I are maximized in certain growth temperature ranges and sub-

sequently decrease with misfit dislocations and with con-

It has recently been noted¹² that numerous III-V alloys exhibit in vapor phase growth spontaneous long-range ordering in the form of monolayer (AC)₁/(BC)₁ superlattices in the (111) orientation (the "CuPt-like structure"). The degree of ordering depends on the growth conditions and is maximized in certain growth temperature ranges and sub-

approximation (LDA), as implemented by the semirelativistic linearized augmented plane-wave (LAPW) method.¹⁵ In all cases we have assumed that the superlattice is matched to a substrate whose lattice constant is the average of its constituents. Table I reveals a substantial

CuPt ordering are given in Ref. 12. In all cases, ordering occurred as a result of homogeneous alloy growth without

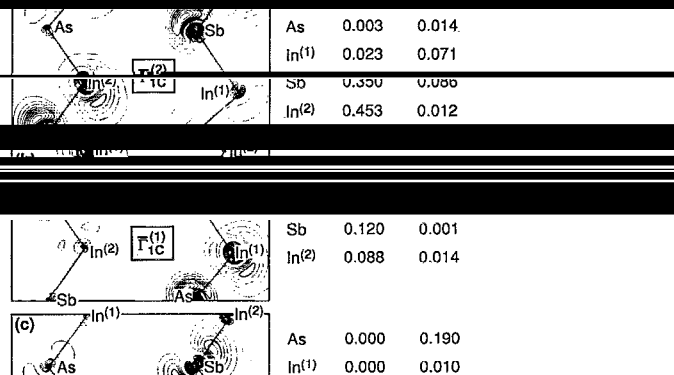
any long-range ordering interactions.

point are constructed from the zincblende-like states at $\langle \Gamma \rangle + \langle L^{111} \rangle$. The folded zincblende states at this wave vector are coupled in the superlattice by the perturbing potential $\delta V(\mathbf{r}) = \delta V^{(\text{chem})} + \delta V^{(\text{size})}$ that has the symme-

try of the superlattice. The resulting superlattice states are coupled to R . This can be exemplified by the results for

size mismatch. This potential couples the alloy states and leads to a "level repulsion" between them, whereby superlattice states are displaced relative to the unperturbed (virtual crystal) states. For example, the $\bar{\Gamma}$ -folding alloy states $\langle \Gamma_{1c} \rangle$ and $\langle L_{1c} \rangle$ couple through δV , producing the superlattice states $\bar{\Gamma}_{1c}^{(1)}$ and $\bar{\Gamma}_{1c}^{(2)}$ that are lowered and raised

The lowering of the CBM will be denoted (Fig. 1) as



produce the superlattice states Γ_{3v} and Γ_{3u} that are also mutually repelled (Fig. 1). The increase in the energy of the VBM will be denoted (Fig. 1) as $\delta^{(2)} = -\epsilon(\Gamma_{1c})$.

imum at X is considerably higher in these systems¹⁴ than $\bar{\Gamma}_{1c}^{(1)}$. The former will not be discussed here.

To quantify the extent of level repulsion, we denote by ΔE^0 the $\langle L_{1c} \rangle - \langle \Gamma_{1c} \rangle$ energy difference before coupling

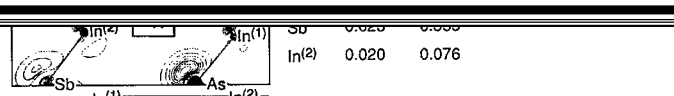


FIG. 2. IV. Coupling of the L_{1c} and Γ_{1c} states in $(\text{InAs})_1(\text{InSb})_1$ in CuPt-like structure, plotted in the (110) plane. The contour step size is 4×10^{-3} e/au.³ Charges are normalized to 2 e/cell. On the right hand side we also give the angular momentum and site decomposed charge (in units of e) for these states, where $\text{In}^{(1)}$ and $\text{In}^{(2)}$

TABLE II. Experimental low-temperature (LT) band gaps for the binary constituents and our predicted semirelativistic LDA-corrected low-temperature direct band gaps [Eq. (4)] for the four systems forming CuPt-like structure. The numbers in parenthesis are crystal field (denoted Δ_{CF} in Fig. 1) averaged values. The last row gives the change in the spin-orbit splitting $\delta\Delta_0$ relative to their respective averaged binary values. To include spin-orbit interactions, subtract $1/3 \delta\Delta_0$ from $E_g(\text{SL})$. All energies are in eV.

	GaAs/InAs	GaSb/InSb	GaAs/InSb	InAs/InSb
$E_g(\text{binary})^a$	1.52/0.42	0.81/0.24	1.52/0.81	0.42/0.24
$E_g(\text{SL})^b$	0.55 (0.58)	0.09 (0.12)	0.27 (0.36)	-0.28 (-0.20)
$\delta\Delta_0$	-0.01	-0.01	0.08	0.08

InAs/InSb: we find that without structural relaxation [where $\delta V(r) = \delta V^{(\text{chem})}(r)$] band coupling gives $R = 0.39$ eV, while after relaxation $\delta V^{(\text{size})}(r)$ further increases R by an additional 0.15 eV.

the various states, as illustrated in Fig. 2 for $(\text{InAs})_x/(\text{InSb})_{1-x}$. We see that each member of a pair of coupling states ($|1/2, +1/2\rangle$ or $|1/2, -1/2\rangle$) has its charge localized on the In–As bonds,

valence-band maximum $\bar{\Gamma}_{3v}^{(2)}$ is found to be localized systematically on the heavy atom semiconductor, while the conduction-band minimum $\bar{\Gamma}_{1c}^{(1)}$ is delocalized over the entire unit cell. The wave functions are localized on the In–As bonds,

given composition x one has additional control over the band gap through variations of the growth parameters that

enhances substantially both the wave function localization and the mixing of s character into the valence-band-edge states [Fig. 2(d)] that are pure p states in the cubic binary constituents. This affects the spin-orbit splitting Δ_0 .¹¹ Our predicted changes in the spin-orbit splitting $\delta\Delta_0 = \Delta_0[(\text{AC})_x(\text{BC})_1] - 1/2 \Delta_0(\text{AC}) - 1/2 \Delta_0(\text{BC})$ are given in Table II. It shows that in the common-anion systems $\delta\Delta_0 \lesssim 0$, while for common-cation systems the negative bowing ($\delta\Delta_0 > 0$) is sizable.

dicted SL gap" $E_g(\text{SL})$ by subtracting the calculated level shifts (Fig. 1) from the experimental¹⁶ (exptl) average of the gaps of the constituents

lower lattice constant than the other partners. Consider

(iii) above would therefore suggest that these SL's will have a larger band gap than the bulk constituent with the small Δ_0 in Table II shows, however, that in all cases except

strong level repulsion that overwhelms other effects. The

energy denominators¹¹ ΔE^0 (Table I), consistent with a perturbation theory description. Indeed, since the L_{1c} level is closer in most alloys to Γ_{1c} than is Γ_{3v} , the level repulsion

D in (111) ST is lower than in (001) ST.

Our semirelativistic calculations predict that in the $(\text{InAs})_x/(\text{InSb})_{1-x}$ system, $(\text{GaAs})_x/(\text{GaSb})_{1-x}$ and $(\text{InAs})_x/(\text{InSb})$, will have direct band gaps of 0.70

the systems are not perfectly ordered. For example, for

given composition x one has additional control over the band gap through variations of the growth parameters that

¹See reviews by R. Triboulet, *Semicond. Sci. Technol.* **5**, 1073 (1990) and in *Materials for Infrared Detectors and Sources*, edited by R. F. C. P. Farren, J. E. Schatzki, and J. T. Cheneau (Materials Research Society, Pittsburgh, 1987), vol. 90.

²B. F. Levine, C. G. Bethea, G. Hasnain, V. O. Shen, E. Pelizzetti, and R. R. Abbott, *Appl. Phys. Lett.* **56**, 851 (1990).

³J. N. Schulman and T. C. McGill, *Appl. Phys. Lett.* **34**, 663 (1979).

⁴D. L. Smith, T. C. McGill, and J. N. Schulman, *Appl. Phys. Lett.* **43**, 180 (1983).

⁵J. Reno and J. P. Faurie, *Appl. Phys. Lett.* **49**, 409 (1986).

Stein, *Appl. Phys. Lett.* **52**, 831 (1988).

⁶D. K. Arch, G. Wicks, T. Tonaue, and J.-L. Staudenmann, *J. Appl. Phys.* **58**, 3933 (1985).

⁷D. L. Smith and C. Mailhiot, *J. Appl. Phys.* **62**, 2545 (1987); C. Mailhiot and D. L. Smith, *J. Vac. Sci. Technol. A* **7**, 445 (1989).

Sci. Technol. B **8**, 710 (1990).

⁸J. T. McDevitt, R. G. Reid, N. A. El-Masry, S. M. DeGan, W. M. Duncan, V. Vir, and E. H. Bell, *Appl. Phys. Lett.* **56**, 1173 (1990).

⁹S.-H. Wei and H. Krakauer, *Phys. Rev. Lett.* **55**, 1200 (1985).

¹⁶*Landolt-Bornstein: Numerical Data and Functional Relationships in Science and Technology*, edited by O. Madelung, M. Schulz, and H. Weiss (Springer, Berlin, 1982), Vol. 17a.

binary constituents (Table II) and $b \approx 0.6$ eV (Ref. 16) is the bowing